RESEARCH ARTICLE

# Figures and figure supplements

Microbiota functional activity biosensors for characterizing nutrient metabolism in vivo

**Darryl A Wesener *et al***

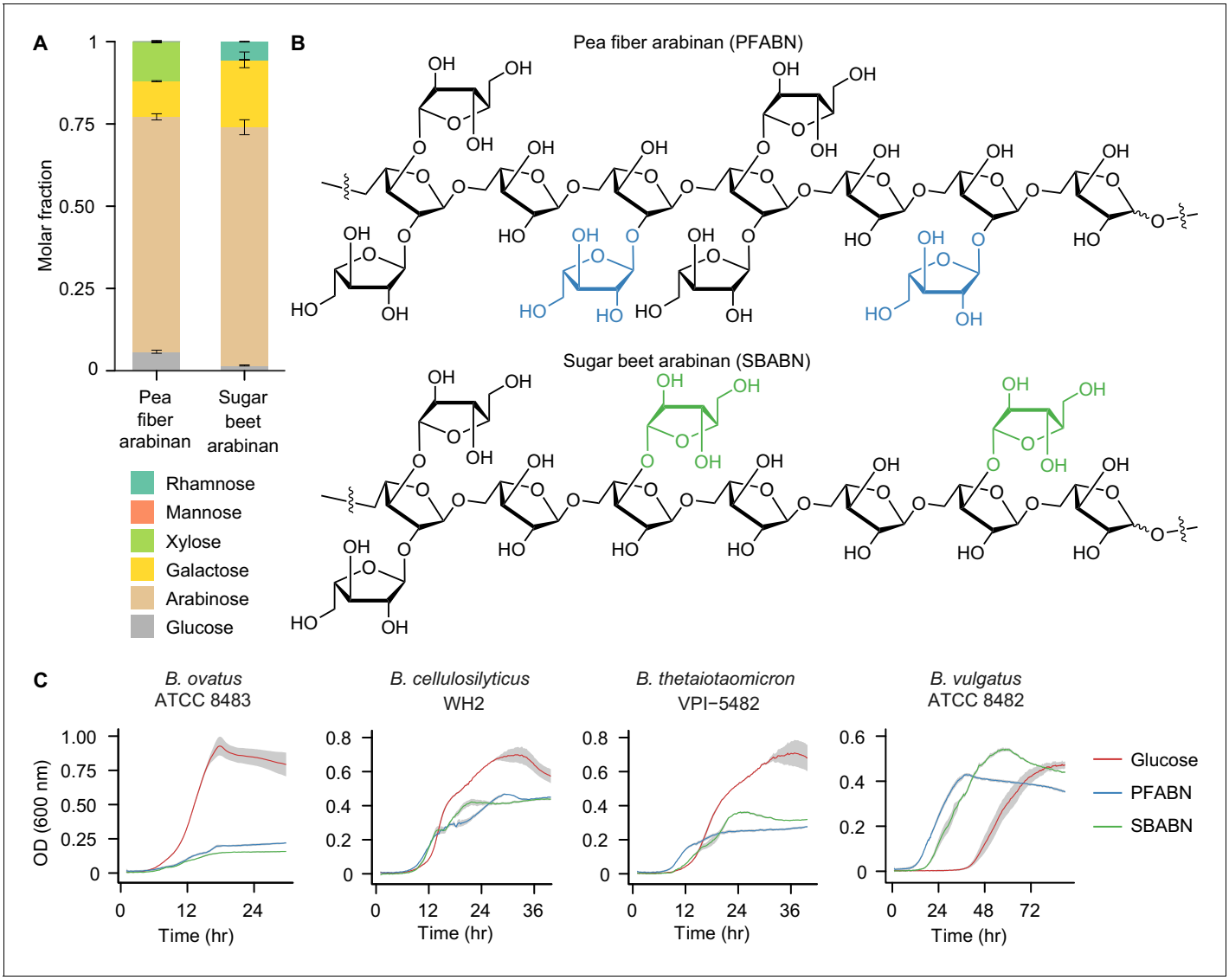


**Figure 1.** Isolation of an arabinose-rich fraction from pea fiber. (**A**) Mole fraction of neutral monosaccharides from PFABN and SBABN. Mean values ± s.d. from triplicate technical measurements are shown. (**B**) Proposed structure of arabinan isolated from pea fiber and sugar beet as determined by glycosyl-linkage analysis. The colored arabinose monosaccharides highlight the different glycosyl branching patterns found in arabinan isolated from the two sources. (**C**) Growth curves of four *Bacteroides* strains cultured in minimal medium containing either glucose or arabinan as the sole carbon source. Data from samples where no exogenous carbon source was added are subtracted from all curves. Solid lines represent the mean and shaded area the s.e.m. of quadruplicate cultures (data shown are representative of 3 independent experiments). (See also ***Supplementary file 1***).

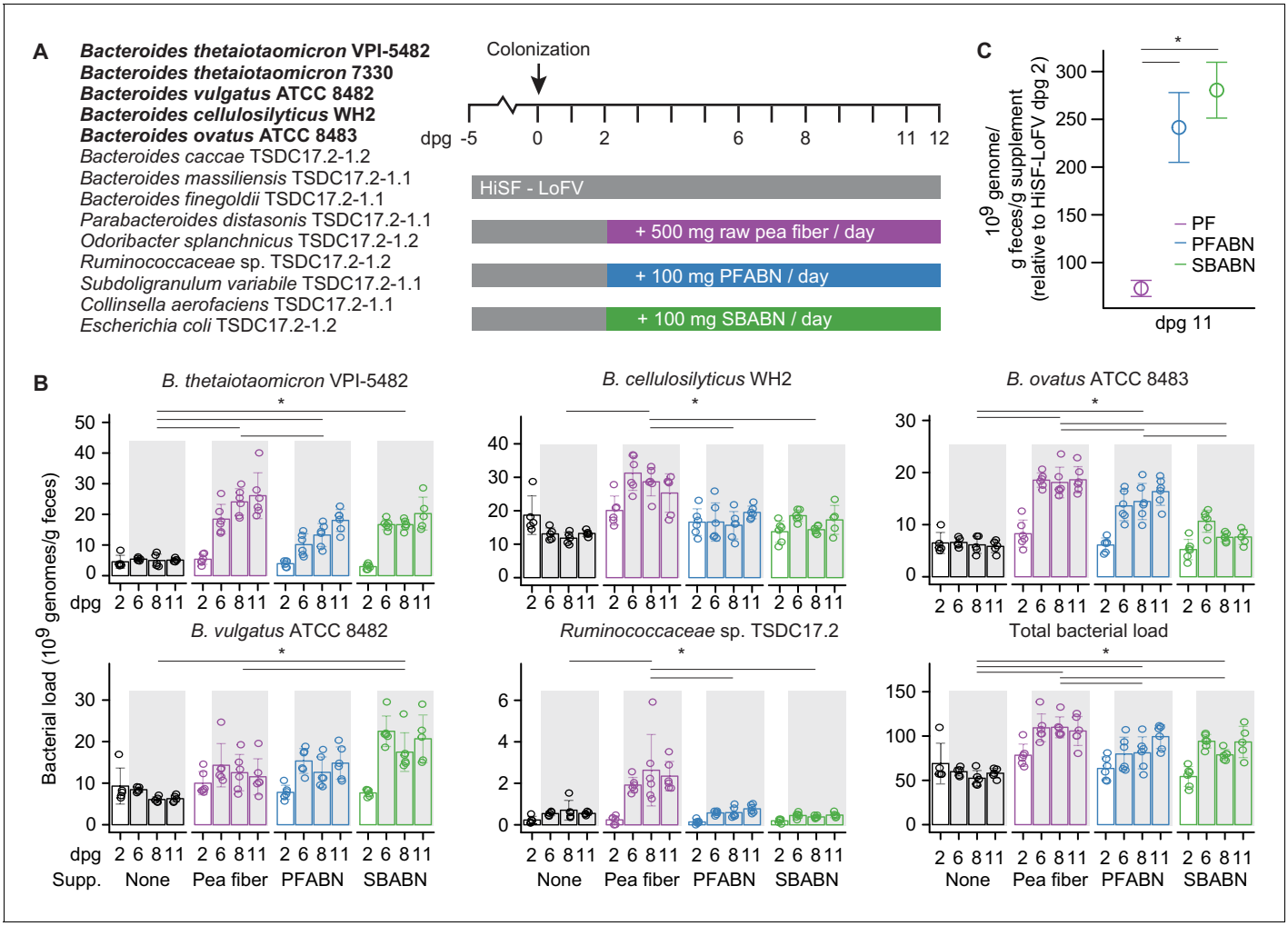


**Figure 2.** Assessing the biological activity of PFABN in gnotobiotic mice colonized with a defined consortium of human gut bacterial strains. (**A**) Experimental design. Germ-free mice were fed the unsupplemented HiSF-LoFV diet for 5 days then colonized with the indicated group of 14 bacterial strains (the five Bacteroides strains represented in the form of Tn mutant libraries are highlighted in boldface). Two days after gavage of the consortium different groups of animals were switched to a HiSF-LoFV diet supplemented with raw pea fiber, PFABN or SBABN and fed that diet monotonously for 10 days (average dose of supplement consumed/per day is shown). Control animals were maintained on the unsupplemented HiSF-LoFV diet. (**B**) Absolute abundances of supplement-responsive bacterial strains, plus the total bacterial load of all 14 strains in fecal samples obtained at the indicated time points (each dot represents a single animal; bar height represents the mean; error bars represent s.d.). *p<0.01 for comparisons denoted by horizontal lines (generalized linear mixed-effects model [Gaussian]; two-way ANOVA with Tukey's HSD, FDR corrected; the data shown are from Experiment two in ***Supplementary file 2*** and are representative of two independent biological experiments). (**C**) Specific activity of each diet supplement on the summed total absolute abundances of the four diet-responsive Bacteroides. Open circles represent mean values and error bars the s.e.m. of two independent biological experiments (n = 10–11 mice/treatment arm). *p<0.01 for comparisons defined by the horizontal lines (generalized linear mixed-effects model [Gaussian]; two-way ANOVA with Tukey's HSD, FDR corrected). (See also ***Supplementary files 2–4***).

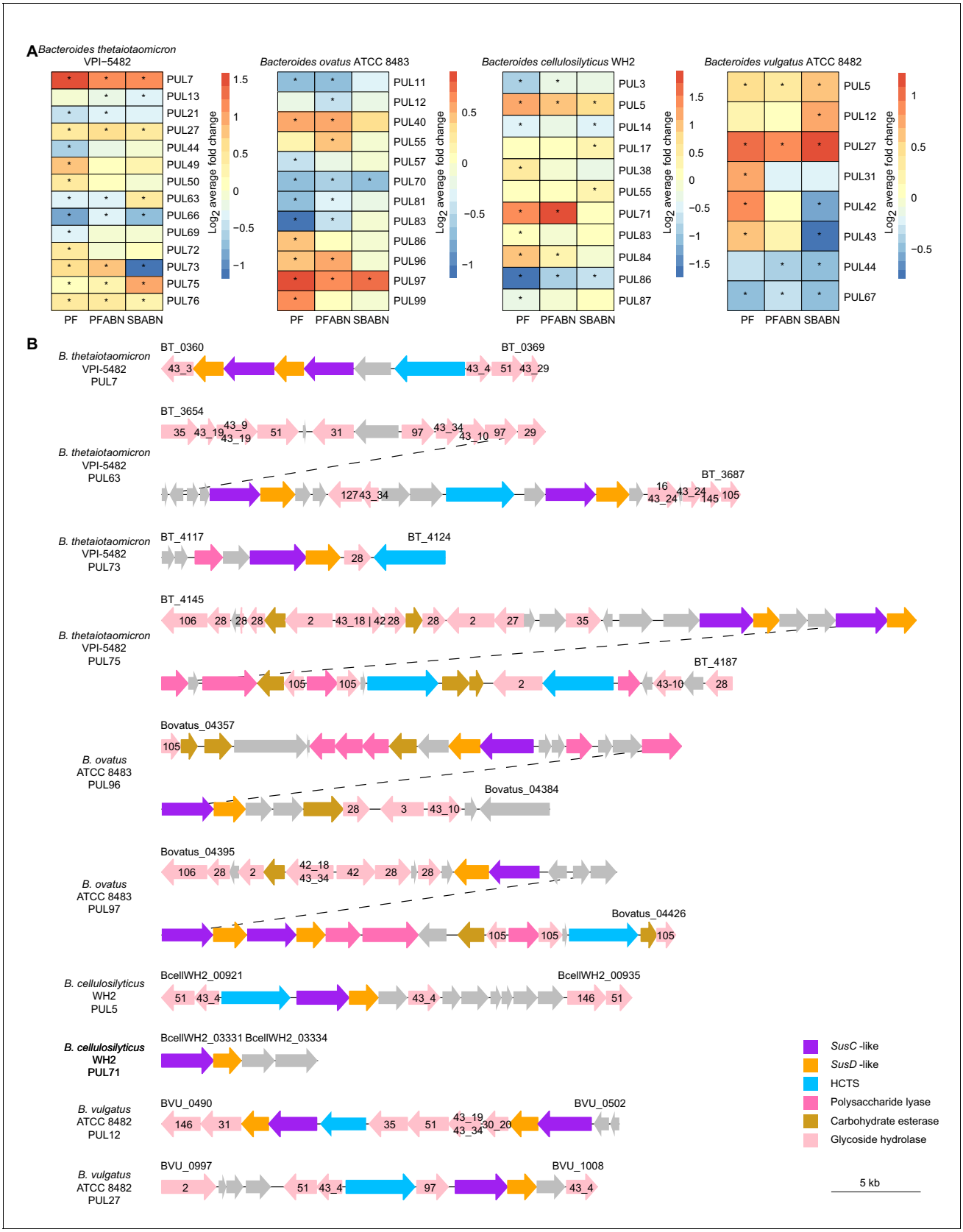


**Figure 2—figure supplement 1.** The effects of supplementing the HiSF-LoFV diet with unfractionated pea fiber, PFABN, or SBABN on PUL gene expression. (**A**) Heat map of the average $\log_2$ fold change in abundance of proteins within PULs identified as supplement-responsive using GSEA.

*Figure 2—figure supplement 1 continued on next page*

*Figure 2—figure supplement 1 continued*

*p<0.05 (unpaired one-sample Z-test, FDR corrected) compared to PUL protein abundance when mice were fed the base HiSF-LoFV diet. (**B**) Organization of supplement-responsive PULs. GH family annotations are included within the colored arrow and are based on PULDB (http://www.cazy.org/PULDB/) accessed on December 6, 2019. Genes denoting the beginning and end of each PUL are noted with their locus tags above the left and right boundaries of the PUL. Dashed lines represent the continuation of a single PUL. PUL annotations and boundaries are identical to those described in ***Patnode et al., 2019***.

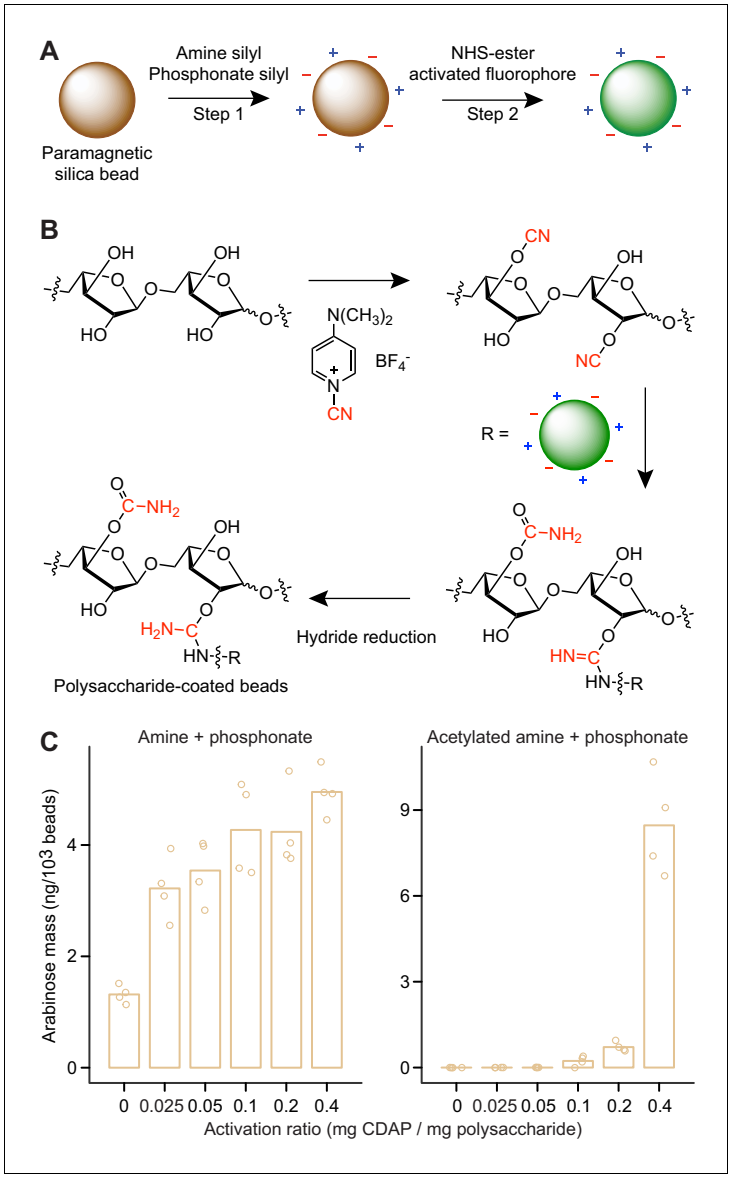


**Figure 3.** Generating microscopic paramagnetic glass beads with covalently attached fluorophores and glycans. (**A**,**B**) Steps used for producing MFABs. The transferred cyano-group from 1-cyano-4-dimethylaminopyridinium tetrafluoroborate (CDAP), and its modification during ligand immobilization are highlighted in red (panel b). Arabinose oligosaccharide is shown as a representative ligand for immobilization. Amine and phosphonate functional groups are denoted by '+' and '–' symbols, respectively. See ***Figure 3—figure supplement 2*** for a more complete depiction of the chemical linkages represented on the surface of an MFAB with bound arabinan. (**C**) Arabinose released during acid hydrolysis from amine plus phosphonate beads with and without surface amine groups acetylated. Beads were coated with SBABN that had been activated using increasing mass ratios of CDAP. Each point represents a single technical measurement (n = 4). Bar height represents the mean value.

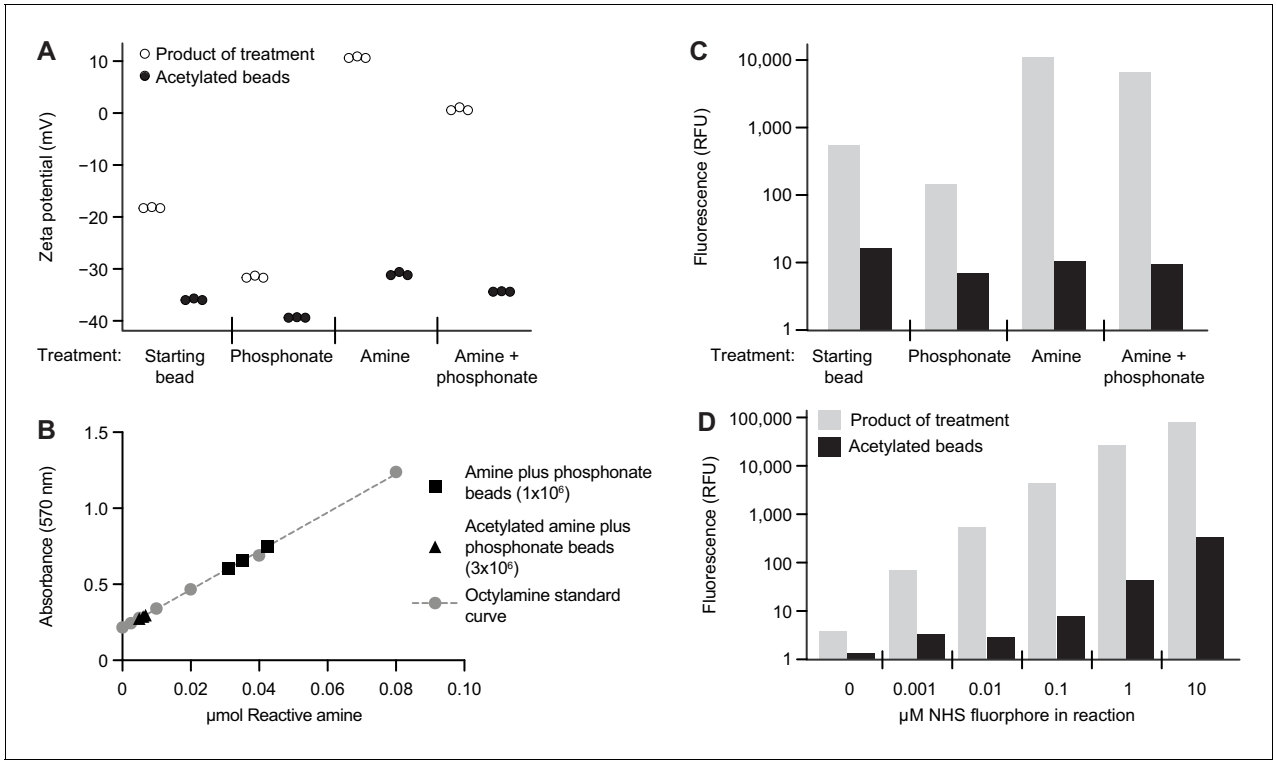


**Figure 3—figure supplement 1.** Characterizing the modified surface chemistry of paramagnetic glass beads. (**A**) Alteration in bead surface zeta potential after modification with organosilanes, with and without amine acetylation. Each point represents the average of at least 12 technical replicate measurements. (**B**) Quantification of reactive surface amine functional groups on amine plus phosphonate beads with and without surface amine acetylation. Octylamine was used to generate a standard curve. Each bead type was analyzed in triplicate. Each point represents a single technical measurement. (**C**) Fluorophore immobilization on the surface of beads after modification with organosilanes, with and without amine acetylation. The height of each bar represents the geometric mean of values obtained from greater than 1000 beads. The concentration of NHS ester-activated fluorophore was 0.1 µM. Results are representative of three independent experiments. (**D**) Level of fluorophore immobilized on an amine plus phosphonate bead after reaction with increasing concentrations of NHS ester-activated fluorophore, with and without bead surface amine acetylation. The height of each bar represents the geometric mean of values obtained from greater than 1000 beads. Results are representative of those obtained in three independent experiments.

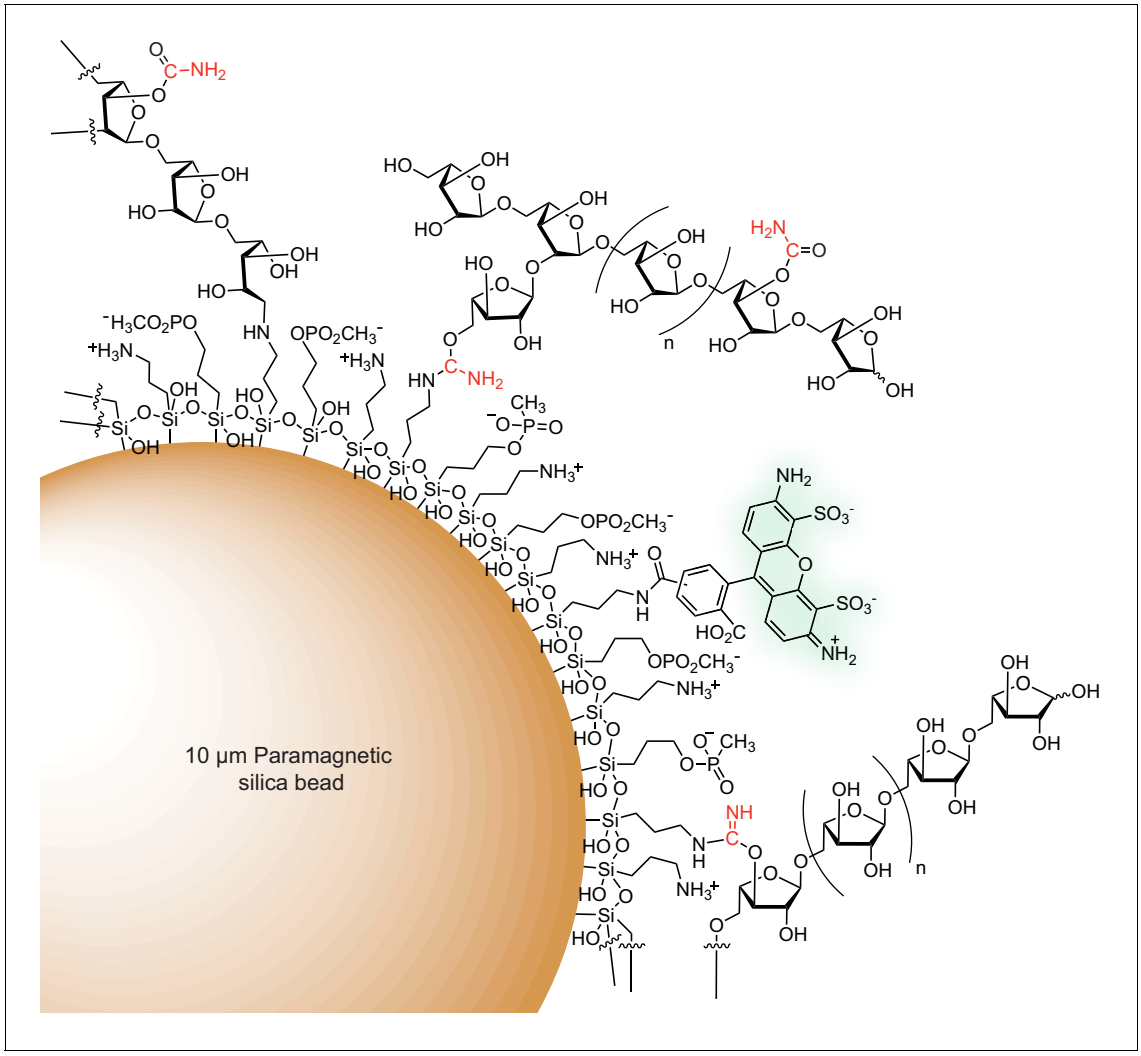


**Figure 3—figure supplement 2.** Schematic of a fluorescent arabinan-coated MFAB. Amine and phosphonate functional groups are covalently attached to the surface of a paramagnetic silica bead via organosilane reagents. Polysaccharide is depicted attached to the bead surface via (1) reductive amination, (2) the product of isourea reduction (an aminal-like linkage), or (3) an isourea bond. An Alexa Fluor 488 (mixed isomer) fluorophore is attached to the bead surface via an amide bond. The product of cyanate-ester hydrolysis, a carbamate, is shown. The carbon and nitrogen atoms from the transferred cyano-group are shown in red.

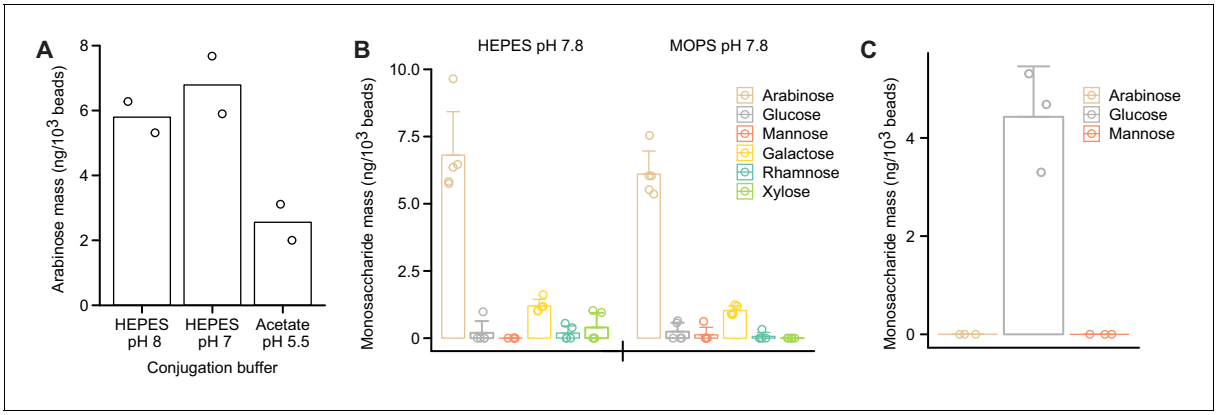


**Figure 3—figure supplement 3.** Conjugation reaction conditions influence immobilization of polysaccharides on the surfaces of the paramagnetic glass beads. (**A**) SBABN subjected to CDAP-based bead immobilization across a range of pH values. Immobilized arabinose was quantified using GC–MS. (**B**) SBABN immobilization in the presence of a HEPES or MOPS-based buffer at an identical pH. Monosaccharides were quantified using GC–MS. (**C**) Maltodextrin oligosaccharide immobilization after CDAP activation. In (**A–C**), each data point represents a single technical measurement while bar heights depict the mean values and error bars the s.d.

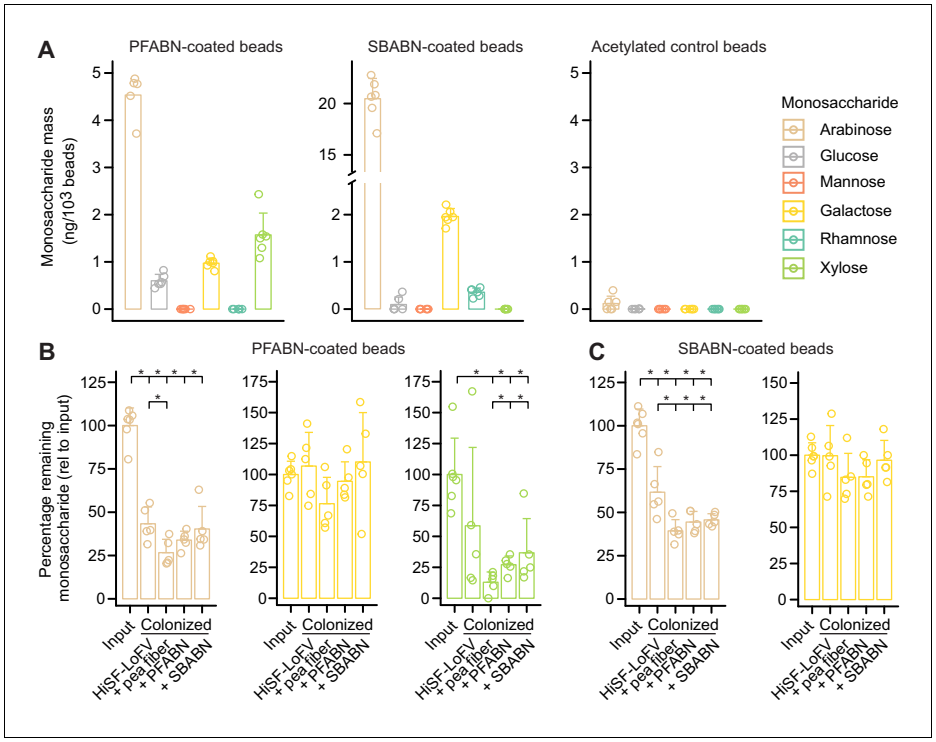


**Figure 4.** Quantifying microbial degradation of PFABN- and SBABN-coated beads in colonized gnotobiotic mice fed unsupplemented or supplemented HiSF-LoFV diets. (**A**) Monosaccharide composition of beads containing covalently bound PFABN or SBABN. Control beads were subjected to surface amine acetylation. The amount of monosaccharide released after acid hydrolysis was quantified by GC-MS. Each point represents a single measurement. Bar height denotes the mean while error bars represent the s.d. (n = 6 biological replicates). (**B**,**C**) Percentage of arabinose, galactose and xylose remaining on the surface of beads recovered from the cecums of mice fed the indicated diets (n = 5 mice/treatment group). Each point represents a single animal. Bar height denotes the mean while error bars represent the s.d. $p<0.05$ (Mann–Whitney U test compared to the group furthest to the left). (See also ***Supplementary file 5***).

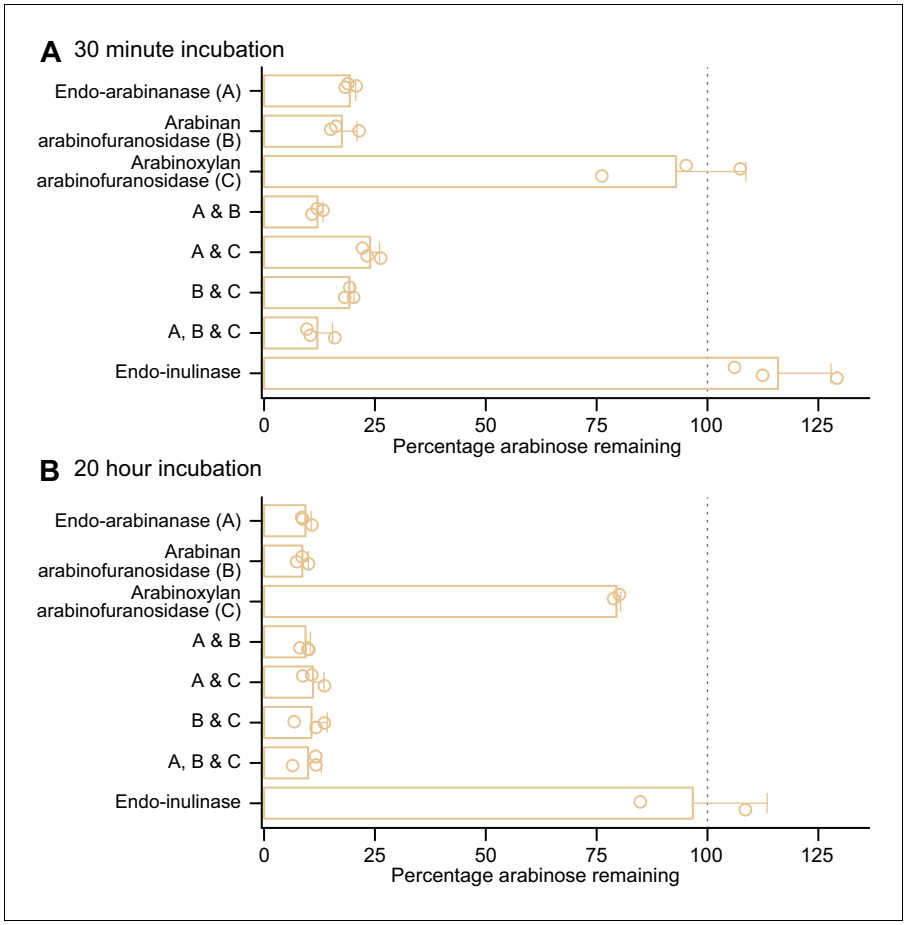


**Figure 4—figure supplement 1.** Enzyme degradation of PFABN immobilized on an MFAB surface using CDAP chemistry. (**A,B**) Soluble glycosyl hydrolases (named and abbreviated as A, B, and C) were added to PFABN-coated MFABs and the fraction of arabinan remaining on the bead surface after 30 min and 20 hr was quantified (by GC–MS). Data are expressed relative to the input preparation of beads that were not exposed to the indicated enzyme alone or to a combination of two or three of the enzymes. Each point represents a single technical measurement (n = 2or three for beads exposed to a single or multiple enzymes). Mean values ± s.d. are plotted. (Note that the modest difference in the amount of bound arabinan remaining on PFABN beads after a 30 min versus a 20 hr incubation with just the commercially available arabinoxylan arabinofuranosidase preparation [enzyme C] is consistent with the fact that it has modest activity against other arabinan polysaccharides.)

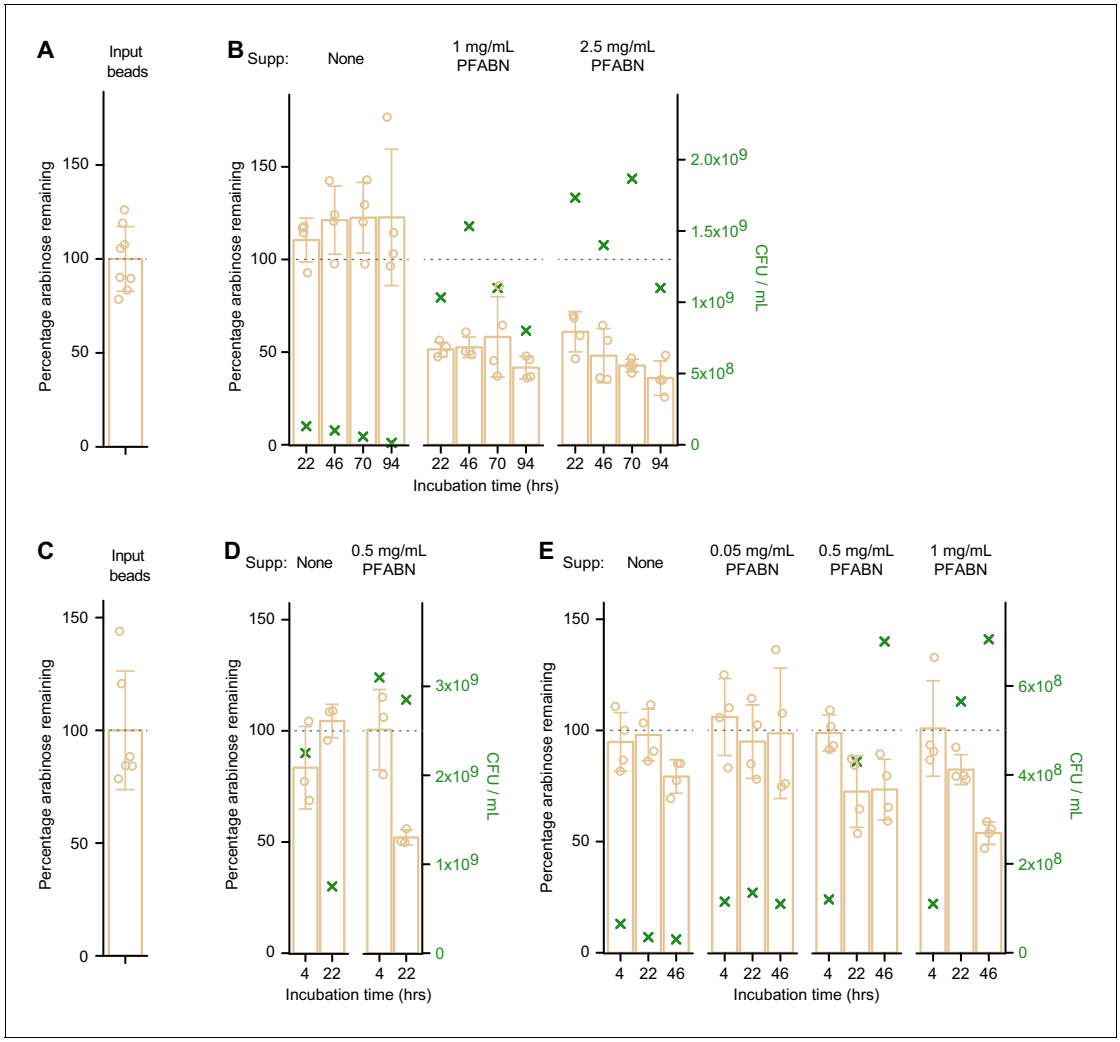


**Figure 4—figure supplement 2.** Degradation of MFAB-bound PFABN by *B. thetaiotaomicron* VPI-5482 and *B. cellulosilyticus* WH2 in vitro. (**A,B**) Input beads (**A**) were incubated with *B. thetaiotaomicron* VPI-5482 that had been grown in BMM medium to mid-log phase with glucose as the carbon source. Cells were harvested and resuspended in BMM with or without different concentrations of supplemented destarched PFABN. PFABN-MFABs were added and the mixture was incubated at 37˚C: aliquots of the reaction mixture were withdrawn at the time points shown (**B**). (**C–E**) Input beads (**C**) were incubated with *B. cellulosilyticus* WH2 that had been grown to mid-log phase in BMM containing glucose (**D**) or PFABN (**E**) as the carbon sources. Cells were harvested and resuspended in BMM with or without different concentrations of destarched PFABN. MFABs were harvested at the indicated time points and the percentage of arabinose remaining on the bead was calculated from the mean absolute mass of arabinose on the input preparation of MFABs used in that experiment. Each point in (**A**) – (**E**) represents a single technical measurement (n = 6 or eight for input beads; 3 or 4 for beads exposed to the Bacteroides strains). Mean values ± s.d. are plotted. The green 'X' denotes the mean number (triplicate technical measurements) of colony forming units (CFU) in the incubation mixture at time of bead harvest (see right y-axis).

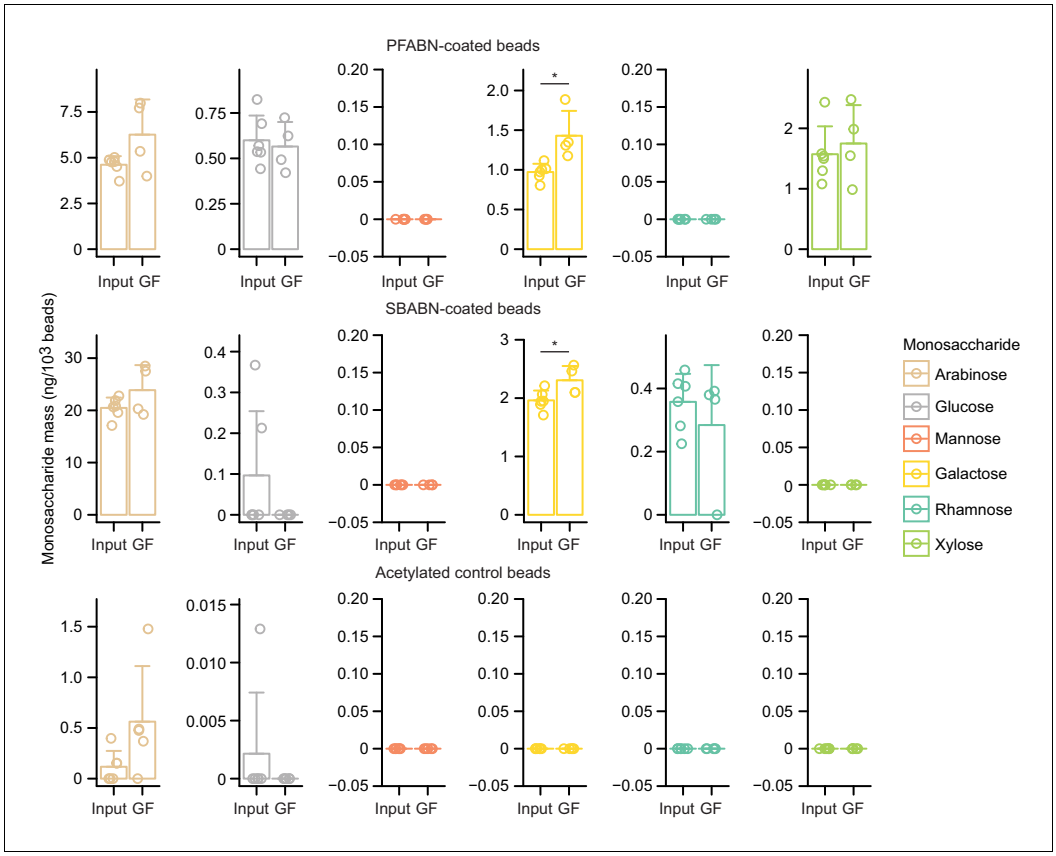


**Figure 4—figure supplement 3.** Assaying whether bead-linked polysaccharides are degraded in germ-free mice. Absolute mass of monosaccharide released from three bead types prior to or after gavage, collection, and purification from germ-free (GF) mice fed the HiSF-LoFV diet supplemented with PFABN. Beads were collected from the cecum 4 hr after gavage. Each point represents a single biological replicate (n = 6 for input beads, four for germ-free animals). Bar height represents the mean while error bars denote the s.d. *p<0.05, Mann–Whitney U test.

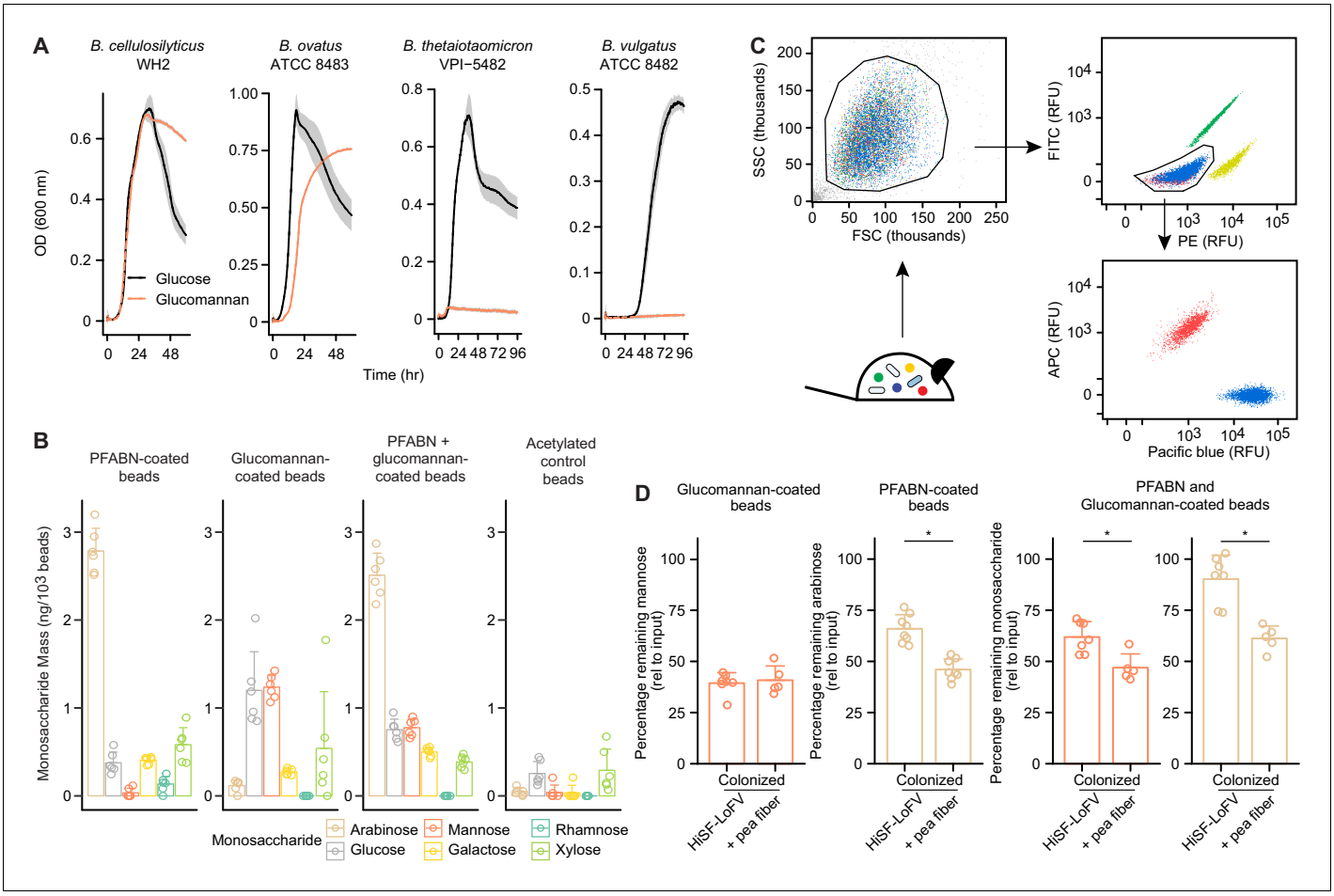


**Figure 5.** Colocalization of PFABN and glucomannan on the same bead results in augmented degradation of glucomannan in gnotobiotic mice colonized with the defined consortium and fed the pea fiber supplemented HiSF-LoFV diet. (**A**) In vitro growth of supplement-responsive Bacteroides species in minimal medium containing glucose or glucomannan as the sole carbon source. Data from samples where no exogenous carbon source was added are subtracted from all curves. The line represents the mean and shaded regions the s.e.m. of quadruplicate measurements. (**B**) Monosaccharide compositions of beads with covalently bound PFABN, glucomannan, or both PFABN and glucomannan. Control beads were subjected to surface amine acetylation. The amount of monosaccharide released after acid hydrolysis was quantified by GC-MS. Each point represents a single measurement. Bar height represents the mean and error bars the s.d. (n = 6 biological replicates). (**C**) Beads containing PFABN alone, glucomannan alone, or both glycans, as well as 'empty' acetylated control beads, each containing a unique fluorophore, were simultaneously introduced by oral gavage into gnotobiotic mice, recovered 4 hr later from their cecums. Each bead-type is subsequently purified by FACS. A representative flow cytometry plot of beads isolated from the cecum is shown. (**D**) Monosaccharide remaining on beads coated with PFABN alone, glucomannan alone, or both glycans after collection and purification from the cecums of mice fed the unsupplemented or pea fiber-supplemented HiSF-LoFV diet. Colors are identical to those used in panel b. The amount of remaining monosaccharide is expressed relative to the absolute mass of monosaccharide immobilized on the surface of each type of input bead. Each point represents a single animal. Bar height represents the mean and error bars the s.d. (n = 5–8 biological replicates). *p<0.05 (Mann–Whitney U test). (See also ***Supplementary file 5***).